Proceedings of the 15th International Heat Transfer Conference, IHTC-15
August 10-15, 2014, Kyoto, Japan

IHTC15-9239

AN INTEGRATED THERMAL ELECTRICAL MODEL FOR SINGLE CELL PHOTOVOLTAIC RECEIVERS UNDER CONCENTRATION

Marios Theristis* **and Tadhg S. O'Donovan**

Institute of Mechanical, Process and Energy Engineering, Heriot-Watt University, Edinburgh, EH14 4AS, United Kingdom

ABSTRACT

Three dimensional finite element analysis is used to predict the cooling requirements of a multijunction photovoltaic cell in steady-state. The inputs to the thermal model are imported through an analytical spectral dependent electrical model which is used to quantify the heat generated in the cell. Both natural convective and radiative heat losses are accounted for all free surfaces to the surroundings. Reflection losses from the cell's surface have also been considered. The results report on the cell's maximum temperature and the heat transfer coefficient required to maintain the cell's temperature below 100°C. In this study, the current density and voltage produced is calculated for each layer, thus the exact thermal power can be quantified giving a more accurate prediction, resulting in a better estimation of the cooling requirements of the system. The results show that the analytical model gives a realistic prediction of the thermal power which passes through each layer of the III-V cell due to its ability to include the current mismatch and the infrared light absorption rate. It is found that CPV single cell configurations up to 500 suns concentration can be adequately cooled passively with a heat sink's thermal resistance below 1.7 K/W while for locations with extreme ambient conditions, a thermal resistance less than 1.4 K/W is needed.

KEYWORDS: Solar energy, Computational methods, Thermal management, Solar spectrum, Multijunction solar cells

1. INTRODUCTION

Concentrating Photovoltaic (CPV) systems use optics to reflect (or refract) Direct Normal Irradiance (*DNI*), concentrating it into a smaller area. High efficiency III-V multijunction (MJ) solar cells can be placed at the focal point receiver to convert the solar energy into electricity. By reducing the semiconductor area, CPV systems can lower the cost of energy [1]. MJ solar cells are made of III-V compound semiconductors and are widely used in space and terrestrial applications. Currently the state-of-art solar cell on the market is the lattice matched three-junction (3J) solar cell made of GaInP/GaInAs/Ge cells [2, 3]. These cells, are monolithically connected in series in a specific way to absorb a larger proportion of the solar spectrum beginning from the shorter wavelengths (GaInP, top cell) to the longer wavelengths (Ge, bottom cell). To date, the highest recorded efficiency for a 3J solar cell is 44.4% [4].

High concentration results in high heat flux on the solar cell's surface and a rapid increase in the cell's temperature. High temperatures reduce the electrical conversion efficiency because of the strong temperature dependence of the open circuit voltage (V_{oc}) and the maximum power voltage (V_{mp}) [5]. It is worth mentioning that under 500x concentration and without any cooling arrangements, the solar cell can heat up to 1400°C [6-9]. This emphasises the need for appropriate cooling technology to decrease the temperature down to safe operation limits to avoid suboptimal performance and risk of system failure.

*Corresponding Author: mt208@hw.ac.uk

Many investigations report on the cooling of CPVs [7, 10, 11]; according to Royne *et al.* [12], who presented an extensive review on different cooling techniques, passive cooling can be sufficient for single cell geometries for solar flux up to 1000 suns where a large area is available below the cell for a heat sink. For densely packed cells and concentrations higher than 150 suns, active cooling is necessary [12]. It was also concluded that the thermal resistance of the cooling system must be less than 10^{-4} m^2K/W for concentration levels above 150 suns. There is also the option to apply active cooling and harness the waste heat for other applications (e.g. domestic heating or industrial process heat) and therefore, to increase an overall system's efficiency. However, due to the parasitic losses, the optimisation of such systems is not straightforward.

MJ solar cells are usually characterised in laboratory facilities under Concentrator Standard Test Conditions (CSTC) (i.e. T_{cell} = 25°C, AM1.5D, *DNI* = 1 kW/m^2), although in the field, the atmospheric conditions can vary significantly. Due to the fact that the layers of the 3J solar cell are monolithically connected and also because of their sensitivity to the spectral variations and intensity of sunlight, the prediction of the electrical and thermal behaviour is still challenging [13]. There also exists a limitation relating to the in-series connection of solar cells; a mismatch in the current produced by each cell will limit the overall output to the lower value; this, in turn will result in greater heat production within the cell. Therefore, by applying a simple *DNI* value as an input in thermal models may give inaccurate results. It is important therefore, to develop smart algorithms, models or methods to realistically determine the electrical performance of the cell to accurately determine the cooling requirements of the system.

Despite the fact that several electrical models for MJ solar cells have been described thoroughly in literature [14-22] which included the spectrum and irradiance dependence, the challenge to develop an integrated TE model which includes the cooling needs is still unsolved. This study presents the methodology of a thermal model which is been developed that uses inputs from a solar spectrum dependent electrical model in order to predict the cooling requirements of a single cell CPV, using the convective heat transfer coefficient as a criterion.

2. DESCRIPTION OF THE MODEL

The heat transfer interface of COMSOL Multiphysics is used to model the thermal behaviour of a MJ solar cell and MATLAB for the electrical performance. These tools offer the "Livelink for MATLAB – COMSOL" interface where the user has the advantage of extending the numerical programming with Finite Element Analysis (FEA) [23].

2.1 Electrical Model

The first step of this methodology is to model the electrical behaviour of a III-V 3J solar cell. AZURSPACE 3C40A [24] was selected for the needs of this study. According to Segev *et al.* [14], the one-diode equivalent circuit model (Fig. 1) is adequate to describe a 3J solar cell in practical applications.

The current-voltage (*I-V*) relationship is given by

$$I_i(V) = I_{0,i}(T_{cell}) \cdot \left(e^{\frac{q \cdot V_i}{n_i \cdot k_B \cdot T_{cell}}} - 1 \right) - I_{SC,i} \tag{1}$$

where *i* is an index for each subcell (1 for top, 2 for middle and 3 for bottom), I_0 the dark saturation current, *q* the elementary charge, *V* the voltage, *n* the diode ideality factor, k_B the Boltzmann constant, T_{cell} the cell's temperature and I_{SC} is the short-circuit current. The dark saturation current density is strongly affected by temperature and is described as

$$J_{0,i}(T_{cell}) = \kappa_i \cdot T_{cell}^{(3+\gamma_i/2)} e^{(-E_{g,i}(T_{cell})/n_i \cdot k_B \cdot T_{cell})} \tag{2}$$

where κ and γ are constants found by regression analysis with experimental data.

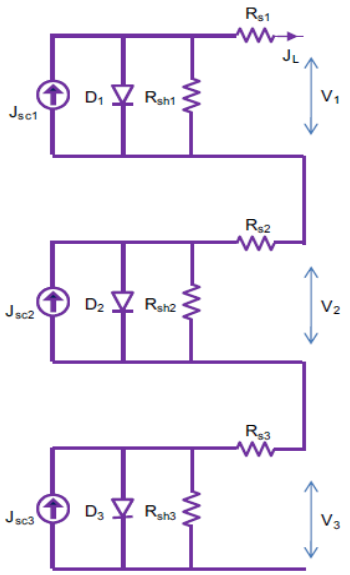

Fig. 1 One-diode equivalent circuit cell model [14].

The energy band gap E_g, is also temperature dependent and is given by the Varshni relation [25]:

$$E_{g,i}(T_{cell}) = E_{g,i}(0) - \frac{\alpha_i \cdot T_{cell}^2}{T_{cell} + \beta_i} \tag{3}$$

where α and β are material dependent constants. If the shunt resistance is sufficiently large to be neglected, then the *I-V* relationship, including the series resistance (R_s), becomes

$$I_i(V) = I_{0,i}(T_{cell}) \cdot \left(e^{\frac{q(V_i - I_i \cdot R_s)}{n_i \cdot k_B \cdot T_{cell}}} - 1 \right) - I_{SC,i} \tag{4}$$

The short-circuit current density for each layer as a function of wavelength is calculated using equation 5:

$$J_{sc,i}(\lambda) = \int_{280}^{\lambda} \frac{q \cdot \lambda \cdot EQE_i(\lambda) \cdot \eta_{opt}(\lambda) \cdot CR \cdot G(\lambda)}{h \cdot c} \cdot d\lambda \tag{5}$$

where q is the elementary charge, λ the wavelength of photons, $EQE_i(\lambda)$ is the External Quantum Efficiency, $\eta_{opt}(\lambda)$ the optical efficiency as a function of wavelength, CR is the concentration ratio, $G(\lambda)$ is the DNI as a function of wavelength, h is the Planck's constant and c the speed of light in vacuum. *EQE* is defined as the ratio of the number of carriers collected by the cell to the number of incident photons.

The total current output due to the series connection is given by

$$I = \min(I_1,\ I_2,\ I_3) \tag{6}$$

The open-circuit voltage for each layer is calculated using:

$$V_{oc,i} = \frac{n_1 \cdot k_B \cdot T_{cell}}{q} \ln\left(\frac{I_{sc,i}}{I_{0,i}(T_{cell})} + 1 \right) \tag{7}$$

The voltage in each junction can be calculated using equation (4):

$$V_i = \frac{n_i \cdot k_B \cdot T_{cell}}{q} \ln\left(\frac{I_{SC,i} - I_i}{I_{0,i}(T_{cell})} + 1 \right) - I_i \cdot R_s \tag{8}$$

The total voltage output is the sum of the voltage in each junction therefore

$$V = \sum_{i=1}^{3} V_i$$
$$V = \frac{k_B \cdot T_{cell}}{q}\left[\sum_{i=1}^{3} n_i \ln\left(\frac{I_{SC,i} - I}{I_{0,i}(T_{cell})} + 1\right)\right] - I \cdot R_s \quad (9)$$

The solar cell's efficiency is defined as the proportion of the maximum power output of the cell to the *DNI* which is incident on the cell:

$$n_{cell} = \frac{P_{out}}{P_{in}} = \frac{P_m}{\int_{280}^{\lambda} CR \cdot A \cdot \lambda \cdot G(\lambda) \cdot n_{opt}(\lambda) \cdot d\lambda} \quad (10)$$

where *A* is the cell's area. Therefore, the heat power produced on the cell is

$$Q_{heat} = P_{in} \cdot (1 - n_{cell}) \cdot (1 - r_{cell}) \quad (11)$$

where r_{cell} is the reflectivity of the cell and is wavelength dependent. It is separated from the optical efficiency which represents the system's optical efficiency and does not include the solar cell's reflections.

2.1 Thermal Model

The configuration of the CPV system used in this study is shown in Fig. 2. The *DNI* is collected by a primary concentrator and a secondary reflector is used for homogenization purposes. The multijunction solar cell is attached to a Direct Copper Bonded (DCB) substrate for heat dissipation and electrical insulation. The heat is transferred by conduction between the solid layers of the receiver. The solar energy that is transformed to heat must be dissipated from the bottom substrate or cooling system to the environment or to another unit. Some heat is lost to the environment, due to natural convection and surface to ambient radiation from all free surfaces.

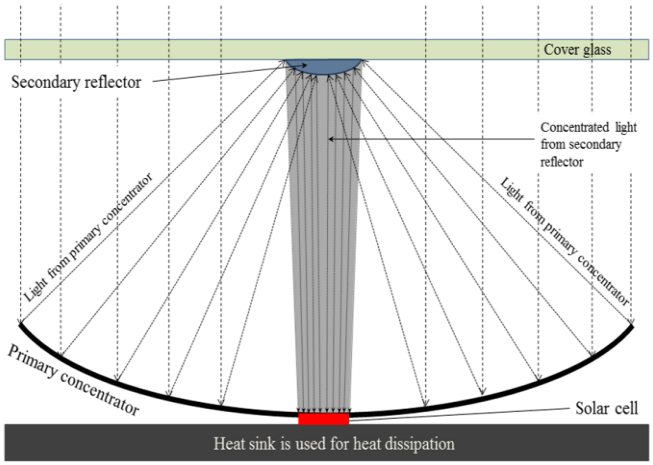

Fig. 2 Configuration of the single cell CPV system [26].

In the case of a passively or actively cooled receiver, the heat is transferred by conduction between the solid layers of the receiver and the steady state equation is given by the Fourier's law of heat conduction:

$$q = -k\nabla T \quad (12)$$

The heat which is dissipated either by natural or forced convection is described by

$$q_{n/f,conv} = h_{n/f} \cdot A \cdot \Delta T \quad (13)$$

The heat, which is lost in the environment, due to natural convection happens on every surface that faces the ambient. COMSOL Multiphysics contains the correlations for each surface orientation (vertical, horizontal or inclined); these can be found in Incropera and DeWitt [27]. The heat that is lost to the environment due to radiation is given by

$$q_{rad} = \varepsilon \cdot \sigma \cdot (\mathrm{T}_{cell}^4 - T_{amb}^4) \tag{14}$$

where ε is the material's emissivity and σ the Stefan-Boltzmann constant. The heat transfer at solids interfaces is defined by the following heat equation to simulate the thermal behaviour:

$$\rho \cdot C_p \frac{\partial T}{\partial t} - \nabla \cdot (k \nabla T) = Q_{heat} \tag{15}$$

where the first term disappears in steady state problems and Q_{heat} is the heat source which is calculated from the electrical model.

3. SIMULATION RESULTS

3.1 Electrical Model

The EQE response of the AZURSPACE 3C40A as characterised by the manufacturer, was used to calculate the solar cell response. As an input for the model, the AM1.5D solar spectrum was taken from the NREL SMARTS model [28]. Assuming that the solar spectrum is uniformly concentrated on the solar cell's surface, all the values of the *DNI* were multiplied by a *CR* of 500x (Fig. 3).

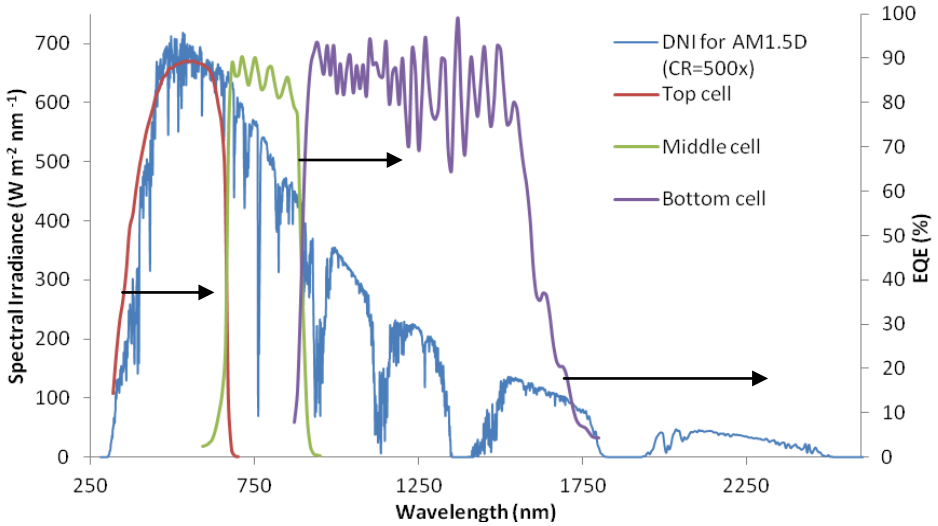

Fig. 3 EQE response for each subcell at 25°C [24] and the AM1.5D solar spectrum from the NREL SMARTS model multiplied by a *CR* of 500x.

Equation (5) gives the short-circuit current density for each subcell as a function of wavelength (Fig. 4). As each layer is connected in series, the total current output of the cell will be restricted to the minimum value of the 3 subcells while the voltage is summed. This has a significant impact on the electrical performance of the cell since the excess current will be transformed directly to heat.

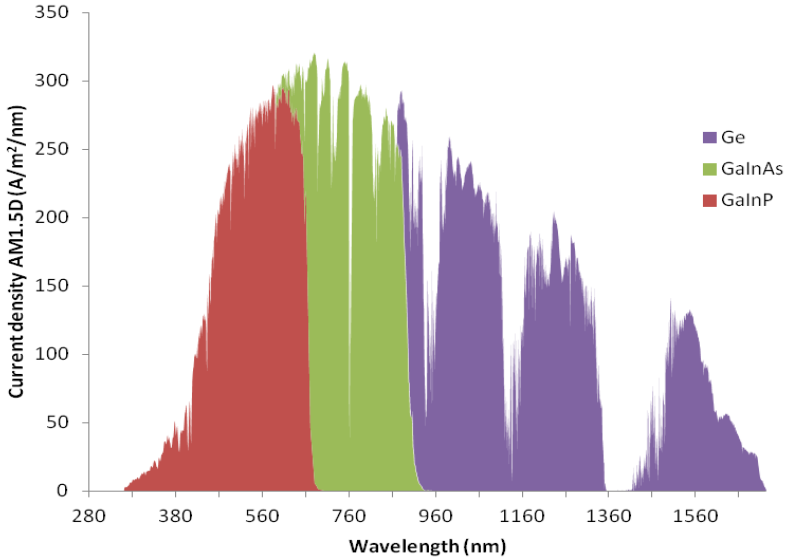

Fig. 4 Short-circuit current density for each layer of the 3J solar cell as a function of wavelength.

In Fig. 5 and 6, the *I-V* and *P-V* curves were plotted for each subcell using the fitting parameters and inputs from Table 1. According to Kinsey *et al.*, [21] the diode's ideality factor is dependent on temperature, however in this study it is assumed to be a constant as well as the EQE_i of each subcell (constant at 25°C). From Fig. 5 and 6, it can be noticed that the excess current from the germanium (cyan curve) is relatively much higher than the other 2 subcells which are almost current matched. The maximum electrical power output from the cell was found to be 13.50 W at 25°C.

Table 1 Solar cell's fitting and input parameters.

Subcell	n	κ (A/cm^{2}K^4)	γ	β (K)	α (eV/K)	E_g at 298 K (eV)	R_s (Ω)	A (cm^2)	n_{opt}	r_{cell}
1	1.9	$5\text{x}10^{-8}$	2	267	$1.7\text{x}10^{-4}$	1.77	0.1	1	0.8	0.01
2	1.45	$6\text{x}10^{-7}$	2	250	$3.1\text{x}10^{-5}$	1.31				
3	1.3	$1\text{x}10^{-5}$	2	235	$6.5\text{x}10^{-5}$	0.69				

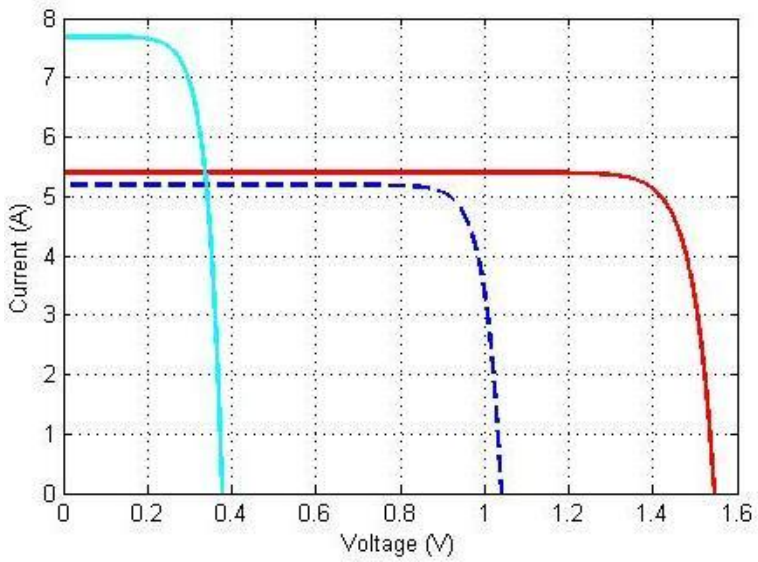

Fig. 5 *I-V* characteristics of Top (red colour), Middle (blue colour) and Bottom subcell (cyan colour).

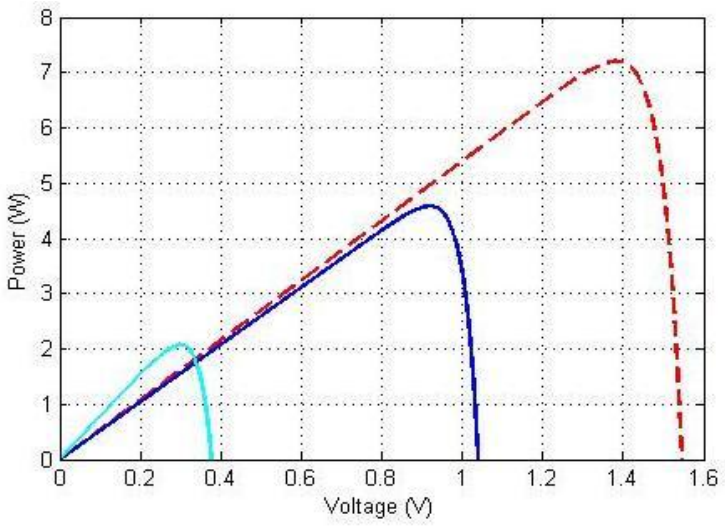

Fig. 6 *P-V* characteristics of Top (red colour), Middle (blue colour) and Bottom subcell (cyan colour).

3.1 Thermal Model

Having calculated the heat input from the solar spectrum dependent electrical model the next step was to apply the values in the thermal model. The geometry and thermal boundary conditions of the model are shown in Fig. 7 and Table 2. Also, the thermophysical properties of the materials used in the 3D model are shown in Table 3. The solar cell is attached on a DCB substrate which is made of copper/Al_2O_3 ceramic/copper. The electrical connections are made of silver. These cells are connected with 2x10A Schottky diodes, however for simplicity, the bypass-diodes, terminals and packing materials are not modelled.

Table 2 Thermal boundary conditions.

No	Region	Boundary Condition
1	Germanium cell	Heat source as found from electrical model
2	All free surfaces on top and sides	Natural convection
3	All free surfaces	Surface to ambient radiation
4	Back plate surface	Natural or forced convection from cooling device
5	All surfaces	Initial temperature (=25°C)

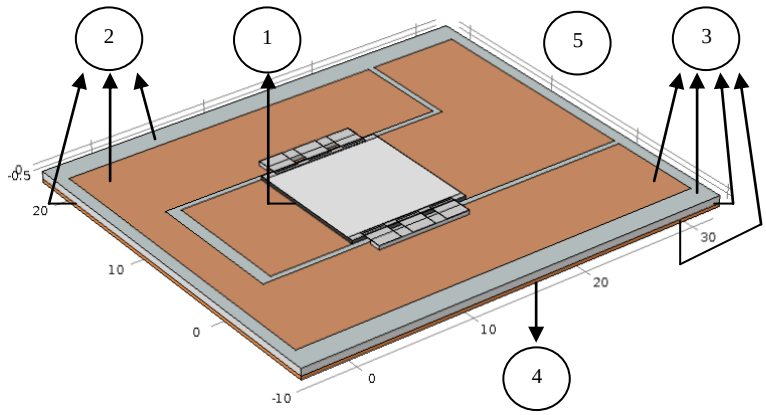

Fig. 7 Geometry and thermal boundary conditions of 3D thermal model.

Table 3 Materials' thermophysical properties.

Layer	k (W/mK)	Cp (J/kgK)	ρ (kg/m^3)
GaInP	73	370	4470
GaInAs	65	550	5316
Ge	60	320	5323
Copper	400	385	8700
Al_2O_3 Ceramic	27	900	3900
Silver	430	235	10490

Since the incident photons with lower energy from $E_{g,i}$ are transmitted to the lower subcell, it is assumed that all the heat will be produced on the bottom subcell (germanium), hence it is modelled as a heat source. All the free areas at the top release heat to the environment through natural convection (≈15 W/m^{2}K) and surface to ambient radiation. The back plate's surface (copper) releases heat to the environment through surface to ambient radiation and also convection where the convective heat transfer coefficient is varied and discussed later on. It is also assumed that the initial temperature is 25°C.

The simulations are conducted in steady state. The electrical model is running for a cell temperature of 25°C and the heat power is then introduced in the 3D thermal model in COMSOL. The cell's temperature found in the thermal model is then imported as an input in the electrical model. The procedure is repeated until a steady state is reached; i.e. $|T_{cell}(s)-T_{cell}(s+1)| \leq 0.002$°C, where s is the number of cycle iterations.

The solar cell manufacturer suggests a maximum cell temperature of 150°C [24], however to avoid long term degradation problems and also the risk of destroying the connections (melting), the solar cell should not operate in excess of 100°C (some other companies suggest up to 120°C) [14]. It is worth mentioning that in high temperatures (over 120°C, 1 sun), the voltage output of the low energy band gap germanium subcell vanishes [29]. Therefore, for the purposes of this study all the cases up to 100°C are examined.

Fig. 8 shows the maximum solar cell's temperature after 6 iterations for convective heat transfer coefficients ranging from 400 W/m^{2}K to 600 W/m^{2}K and a constant ambient temperature of 25°C (T_{amb}). The steady state in all cases is achieved after the 3rd iteration.

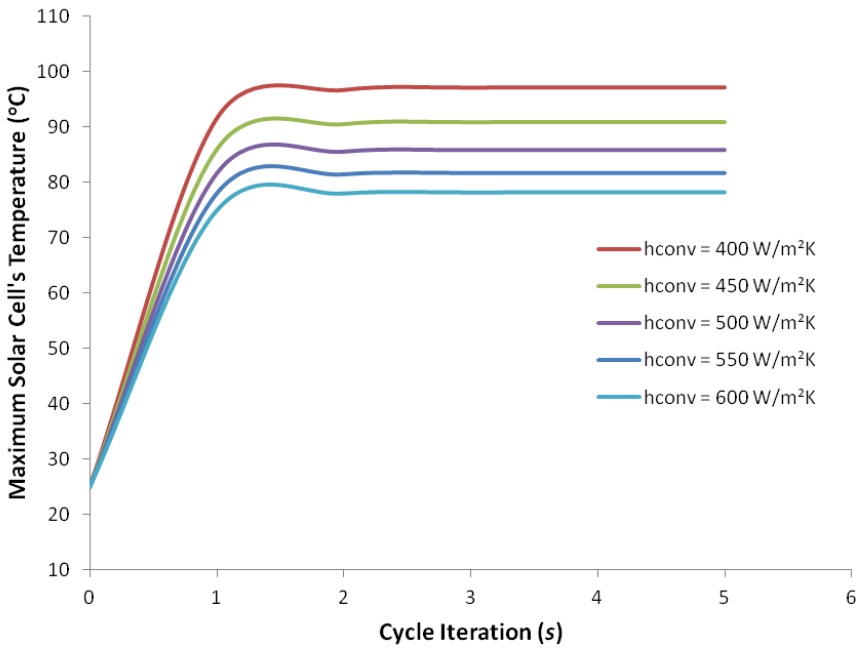

Fig. 8 Maximum solar cell's temperature as a function of the cycle iteration, s.

In Fig. 9, the solar cell's temperature is estimated for 400 W/m^{2}K ≤ h_{conv}≤ 600 W/m^{2}K and 25°C ≤ T_{amb} ≤ 45°C. Ambient temperature has a strong influence on the cell's temperature, however it is shown that for locations with high *DNI* and extreme ambient temperatures, passive cooling of R_{th} ≤ 1.4 K/W can be sufficient to maintain the cell below a safe operation limit. For locations with ambient temperature lower than 40°C, a higher heat sink thermal resistance may be acceptable. According to Lee [30], the performance range of heat sinks via natural convection is between 1.2 - 12 K/W therefore, since the back surface area of the receiver is 32x37 mm, it can be concluded that passive cooling is adequate for single cells under concentrations up to 500 suns.

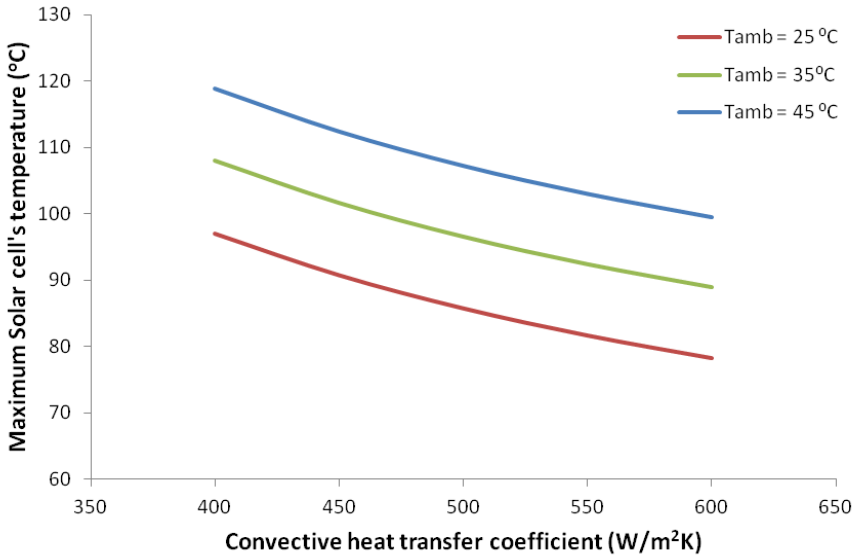

Fig. 9 Maximum solar cell's temperature as a function of the convective heat transfer coefficient for 25°C≤T_{amb}≤45°C.

Fig. 10 shows the temperature distribution across the 3J solar cell for h_{conv} = 700 W/m^{2}K (i.e. 1.2 K/W) and T_{amb} = 45°C. A maximum temperature of 94°C is observed in the centre of the cell while the temperature of the top layer of the DCB board, which is not illuminated, is from 65°C at the edges to 80°C near the cell.

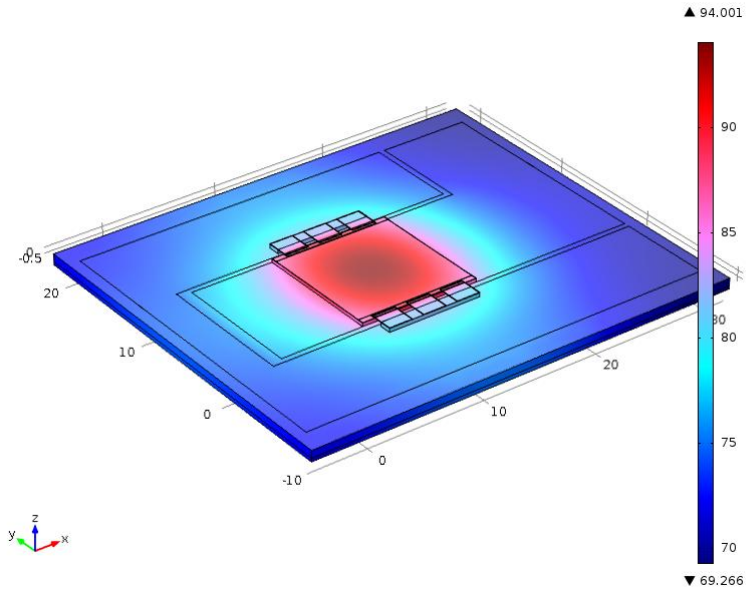

Fig.10 Temperature distribution (°C) across the solar cell's assembly for h_{conv} = 700 W/m^{2}K and T_{amb} = 45°C.

4. CONCLUSIONS & DISCUSSION

An integrated solar spectrum dependent TE model is described for a 3J solar cell under concentration of 500 suns. This model can lead to the accurate quantification of the thermal power which needs to be dissipated, including the excess thermal output due to current mismatch.

It is found that CPV single cell configurations can be adequately cooled passively with a heat sink's thermal resistance below 1.7 K/W while for locations with extreme ambient conditions, a thermal resistance less than 1.4 K/W is needed.

Despite the interesting conclusions that can be drafted from the aforementioned results, this integrated TE numerical model, needs to be further improved. First of all, since the solar spectrum is transient during the day, the AM1.5D does not offer representative results of the realistic operation of the solar cell in the field. More solar spectrums need to be added in order to examine the influence of solar spectrum, irradiance, ambient temperature on the cooling requirements.

The *EQE*, which was taken as a constant in this study, is strongly temperature dependent, where with increasing temperature, thus decreasing energy band gap, it tends to shift towards the higher wavelengths [3, 19, 20, 31]. Therefore the next step is to add the *EQE* temperature dependence.

This study investigates the thermal behaviour of a solar cell assembly; however the concentrator optics and cover glass are not modelled in terms of their transmissivity or reflectivity as a function of wavelength and incidence angle. This will further increase the accuracy of the incident solar flux on the solar cell's surface calculation.

ACKNOWLEDGMENT

This research is part of the BioCPV project [32], which will develop a small scale power plant by integrating Concentrating Photovoltaics (CPV) with biomass and hydrogen generation in order to help to reduce the urban and rural energy divide in India. The authors acknowledge the support of the Engineering and Physical Sciences Research Council (EPSRC), UK and the Department of Science and Technology, India for funding the BioCPV project. The authors would also like to thank AZURSPACE Solar Power GMBH and in particular Mr Bensch Werner for providing the *EQE* data of the 3C40A 3J solar cell.

NOMENCLATURE

A	area	(m^2)	n	diode ideality factor	(-)
c	speed of light in vacuum	(m/s)	n_{cell}	solar cell's efficiency	(-)
C_p	heat capacity	(J/kg·K)	n_{opt}	optical efficiency	(-)
CR	concentration ratio	(-)	P_{in}	incident power	(W)
DNI	direct normal irradiance	(W/m^2)	P_m	maximum power output	(W)
EQE	external quantum efficiency	(-)	q	elementary charge	(C)
E_g	energy band gap	(eV)	Q_{heat}	heat power	(W)
$G(\lambda)$	spectral DNI	(W/m^2/nm)	r_{cell}	solar cell's reflectivity	(-)
h	Planck's constant	(J·s)	R_s	series resistance	(Ω)
h_{conv}	conv. heat transfer coeff.	(W/m^2K)	R_{th}	thermal resistance	(K/W)
I	current	(A)	T_{amb}	ambient temperature	(°C)
I_{sc}	short-circuit current	(A)	T_{cell}	solar cell's temperature	(°C)
I_0	dark saturation current	(A)	V	voltage	(V)
J_0	dark saturation current density	(A/m^2)	V_{oc}	open circuit voltage	(V)
k	thermal conductivity	(W/m·K)			
k_B	Boltzmann constant	(eV/K)			

Greek letters					
α	material dependent constant	(eV/K)	ε	emissivity	(-)
β	material dependent constant	(K)	κ	constant*	(A/cm^2K^4)
γ	constant*	(-)	λ	wavelength	(nm)
ΔT	temperature difference	(°C)	ρ	density	(kg/m^3)
			σ	Stefan-Boltzmann constant	(W/m^2K^4)

* Found by regression analysis

REFERENCES

[1] M. G. Liu, G. S. Kinsey, W. Bagienski, A. Nayak, and V. Garboushian, "Indoor and Outdoor Comparison of CPV III-V Multijunction Solar Cells," *IEEE Journal of Photovoltaics*, vol. 3, pp. 888-892, Apr 2013.

[2] W. Guter, J. Schone, S. P. Philipps, M. Steiner, G. Siefer, A. Wekkeli, E. Welser, E. Oliva, A. W. Bett, and F. Dimroth, "Current-matched triple-junction solar cell reaching 41.1% conversion efficiency under concentrated sunlight," *Applied Physics Letters*, vol. 94, Jun 1 2009.

[3] H. Helmers, M. Schachtner, and A. W. Bett, "Influence of temperature and irradiance on triple-junction solar subcells," *Solar Energy Materials and Solar Cells*, vol. 116, pp. 144-152, 2013.

[4] *NREL: National Center for Photovoltaics, http://www.nrel.gov/ncpv/images/efficiency_chart.jpg, [Accessed March 31, 2014]*.

[5] H. Cotal and R. Sherif, "Temperature dependence of the IV parameters from triple junction GaInP/InGaAs/Ge concentrator solar cells," *Conference Record of the 2006 IEEE 4th World Conference on Photovoltaic Energy Conversion, Vols 1 and 2*, pp. 845-848, 2006.

[6] A. Y. Kuo, B. Lin, C. C. Huang, J. Chen, P. K. Chiang, S. Shao, R. Wu, and I. Lin, "A Modular Solar Engine with Solar Cell, Heat Pipe, and Heat Sink in an Integrated Package for High Concentrating Photovoltaic," in *34th IEEE PVSC*, 2009, pp. 166-169.

[7] K. Araki, H. Uozumi, and M. Yamaguchi, "A simple-passive cooling structure and its heat analysis for 500 X concentrator PV module," in *29th IEEE PVSC*, 2002, pp. 1568-1571.

[8] C. Min, C. Nuofu, Y. Xiaoli, W. Yu, B. Yiming, and Z. Xingwang, "Thermal analysis and test for single concentrator solar cells," *Journal of Semiconductors*, vol. 30, 2009.

[9] Z. B. Ye, Q. F. Li, Q. Z. Zhu, and W. G. Pan, "The cooling Technology of Solar Cells under Concentrated system," *6th IEEE IPEMC*, vol. 1-4, pp. 1252-1256, 2009.

[10] T. L. Chou, Z. H. Shih, H. F. Hong, C. N. Han, and K. N. Chiang, "Thermal Performance Assessment and Validation of High-Concentration Photovoltaic Solar Cell Module," *IEEE Transactions on Components Packaging and Manufacturing Technology*, vol. 2, pp. 578-586, Apr 2012.

[11] S. K. Natarajan, T. K. Mallick, M. Katz, and S. Weingaertner, "Numerical investigations of solar cell temperature for photovoltaic concentrator system with and without passive cooling arrangements," *International Journal of Thermal Sciences*, vol. 50, pp. 2514-2521, Dec 2011.

[12] A. Royne, C. J. Dey, and D. R. Mills, "Cooling of photovoltaic cells under concentrated illumination: a critical review," *Solar Energy Materials and Solar Cells*, vol. 86, pp. 451-483, Apr 1 2005.

[13] M. Steiner, G. Siefer, A. Bosch, T. Hornung, and A. W. Bett, "Realistic Power Output Modeling Of CPV Modules," *8th International Conference on Concentrating Photovoltaic Systems (Cpv-8)*, vol. 1477, pp. 309-312, 2012.

[14] G. Segev, G. Mittelman, and A. Kribus, "Equivalent circuit models for triple-junction concentrator solar cells," *Solar Energy Materials and Solar Cells*, vol. 98, pp. 57-65, 2012.

[15] E. F. Fernández, F. Almonacid, P. Rodrigo, and P. Pérez-Higueras, "Model for the prediction of the maximum power of a high concentrator photovoltaic module," *Solar Energy*, vol. 97, pp. 12-18, 2013.

[16] E. F. Fernandez, G. Siefer, F. Almonacid, A. J. G. Loureiro, and P. Perez-Higueras, "A two subcell equivalent solar cell model for III-V triple junction solar cells under spectrum and temperature variations," *Solar Energy*, vol. 92, pp. 221-229, Jun 2013.

[17] P. Rodrigo, E. Fernández, F. Almonacid, and P. Pérez-Higueras, "Models for the electrical characterization of high concentration photovoltaic cells and modules: A review," *Renewable and Sustainable Energy Reviews*, vol. 26, pp. 752-760, 2013.

[18] A. Ben Or and J. Appelbaum, "Estimation of multi-junction solar cell parameters," *Progress in Photovoltaics*, vol. 21, pp. 713-723, Jun 2013.

[19] G. Siefer and A. W. Bett, "Analysis of temperature coefficients for III–V multi-junction concentrator cells," *Progress in Photovoltaics: Research and Applications*, pp. n/a-n/a, 2012.

[20] G. S. Kinsey and K. M. Edmondson, "Spectral Response and Energy Output of Concentrator Multijunction Solar Cells," *Progress in Photovoltaics*, vol. 17, pp. 279-288, Aug 2009.

[21] G. S. Kinsey, P. Hebert, K. E. Barbour, D. D. Krut, H. L. Cotal, and R. A. Sherif, "Concentrator multijunction solar cell characteristics under variable intensity and temperature," *Progress in Photovoltaics*, vol. 16, pp. 503-508, Sep 2008.

[22] C. Dominguez, I. Anton, and G. Sala, "Multijunction solar cell model for translating I-V characteristics as a function of irradiance, spectrum, and cell temperature," *Progress in Photovoltaics*, vol. 18, pp. 272-284, Jun 2010.

[23] *COMSOL Multiphysics FEA Software [Details at: http://www.comsol.com/]*.

[24] *AZURSPACE Solar Power GMBH, http://azurspace.de/images/pdfs/CPV%20TJ%20Solar%20Cell%203C40A%2032x37mm.pdf, [Accessed December 5, 2013]*.

[25] Y. Varshni, "Temperature dependence of the energy gap in semiconductors," *Physica*, vol. 34, pp. 149-154, 1967.

[26] M. Theristis, G. E. Arnaoutakis, N. Sarmah, T. K. Mallick, and T. S. O'Donovan, "Solar spectrum dependent thermal model for HCPV systems," in *13th UK Heat Transfer Conference*, London, 2013.
[27] F. P. Incropera and D. P. DeWitt, *Fundamentals of Heat and Mass Transfer*, Fourth Edition ed. New York: John Wiley & Sons, 1996.
[28] C. A. Gueymard, "Parameterized transmittance model for direct beam and circumsolar spectral irradiance," *Solar Energy*, vol. 71, pp. 325-346, 2001.
[29] K. Nishioka, T. Takamoto, T. Agui, M. Kaneiwa, Y. Uraoka, and T. Fuyuki, "Evaluation of temperature characteristics of high-efficiency InGaP/InGaAs/Ge triple-junction solar cells under concentration," *Solar Energy Materials and Solar Cells*, vol. 85, pp. 429-436, Jan 31 2005.
[30] S. Lee, "Optimum design and selection of heat sinks," *Eleventh Annual IEEE Semiconductor Thermal Measurement and Management Symposium*, pp. 48-54, 1995.
[31] D. Aiken, M. Stan, C. Murray, P. Sharps, J. Hills, and B. Clevenger, "Temperature dependent spectral response measurements for III-V multi-junction solar cells," *Conference Record of the Twenty-Ninth Ieee Photovoltaic Specialists Conference 2002*, pp. 828-831, 2002.
[32] *BioCPV Website, http://biocpv.ex.ac.uk, [Accessed December 4, 2013]*.